Direct hydrocarbon detection (DHI) techniques for prospective exploration targets in Chaoshan Depression

Direct hydrocarbon detection (DHI) techniques for prospective exploration targets in Chaoshan Depression

Guangjian Zhong[1, 2, 5], Renqi Jiang[3], Hai Yi[1, 2], Jincai Wu[3], John Castagna[4], Changmao Feng[1, 2], Gang Zhou[3], Kun Wang[3], Lina Liu[3] and Ming Sun[1, 2]

[1]Key Laboratory of Marine Mineral Resources, Ministry of Natural Resources, Guangzhou, China
[2]Guangzhou Marine Geological Survey, Guangzhou, Guangdong, China
[3]New Horizons Ltd., Beijing, China
[4]University of Houston, Houston, United State of American

[5]Corresponding author's e-mail: 2645078906@qq.com

Abstract. Located in northern South China Sea, Pearl River Mouth Basin is a large Meso-Cenozoic basin. And in southeasters part of the basin lies Chaoshan Depression, which is mainly a residual Mesozoic depression, with a construction of Meso-Cenozoic strata over 7000m thick and good hydrocarbon accumulation conditions. The selected DHI technique, amplitude attribute of -90 degree phase component derived by phase decomposition is employed to the zone of interest (ZOI) of B structure, Chaoshan Depression. And it is found that there are evident amplitude anomalies occurring around ZOI of structure B. Phase decomposition is applied to forward modelling results of the ZOI, and high amplitudes occur on the -90 degree phase component more or less when ZOI is charged with hydrocarbon, which shows that the amplitude abnormality in ZOIs of structure B is probably caused by oil and gas accumulation. Meanwhile, another DHI attribute of spectral decomposition peak amplitude is applied also to ZOIs of B structure, and there is also amplitude anomalies coincides with those of -90 degree phase component. The two DHI attributes' coincidence strengthens the confidence of hydrocarbon accumulation prediction results.

1. Introduction

The Chaoshan Depression is located in the southeast of the Pearl River Mouth Basin, northern South China Sea, with an area of more than 3.7×10^4 km^2 and a water depth ranging from 300m to 2000m. China National Offshore Oil Corporation conducted seismic surveys and preliminary studies in the region from 1979 to 1986. With the continuous oil and gas exploration in the Pearl River Mouth Basin [1] and in order to search for new exploration areas, detailed studies of the Chaoshan Depression began in the early 1990s, and it was found that the lower tectonic layers of the Chaoshan Depression were Mesozoic marine sediments, with the largest thickness of about 7000m, which has the potential to generate hydrocarbons and the conditions to form various types of oil and gas traps [2-13].

The Chaoshan Depression is a residual Mesozoic depression, which experienced mid-late Jurassic subsidence, late Jurassic to early Cretaceous uplift, superimposed burial of early to late Cretaceous, and then late Cretaceous Uplift and erosion. The Guangzhou Marine Geological Survey Bureau divided the Chaoshan Depression into five secondary tectonic units, namely Eastern Sag, Western Sag, Central Low Uplift, Northern Slope, Central Slope and Western Slope. Among them, B Structure in Central Low

Uplift is selected as a favourable exploration target, (Figure 1). The article will elaborate on petroleum potential and DHI analysis of the target.

Due to the shortage of available drilling data, reliable petro physical data and hydrocarbon information in the target area of the Chaoshan Depression (Figure 1), there is a large uncertainty in the direct prediction of oil and gas with conventional techniques. In order to make a breakthrough to the situation of Mesozoic oil and gas exploration in the Chaoshan Depression, this study applies peak frequency amplitude attribute and phase decomposition amplitude attribute analysis techniques for direct oil and gas detection.

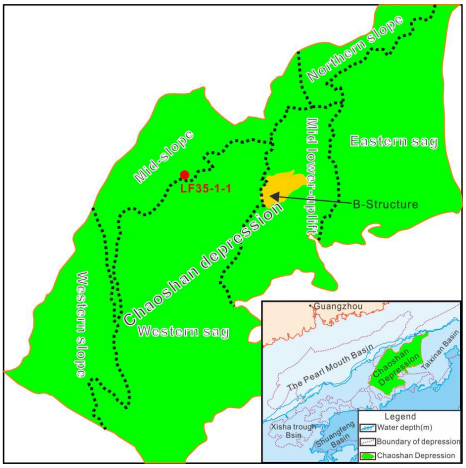

Figure 1. The location map of the favourable target (Structure B) in Chaoshan Depression.

2. Petroleum geology conditions in Chaoshan Depression

Drilled well LF35-1-1 confirmed that Chaoshan Depression is filled with Cretaceous continental sediments and Middle-Late Jurassic marine sediments, among which Middle-Late Jurassic marine sediments have good petroleum geological conditions [14-16].

2.1. Source rocks

The upper part of the Middle-Upper Jurassic strata revealed by well LF35-1-1 is composed of grey-black veined layered mudstone, argillaceous siltstone with siliceous rock, containing a small amount of micrite limestone; the lower part is grey-black veined layered mudstone and shale siltstone with sandstone, limestone. The mudstones are rich in organic debris. A set of river-lake sediments is generally made up of the Cretaceous strata. The upper part is a combination of purple mudstone, siltstone and sandstone with a small amount of marl, and the lower part is a combination of grey grained layered mudstone, siltstone and sandstone, containing some organic debris (Table 1).

Table 1. Dark mud-rock properties at well LF35-1-1.

Interval (m)	Strata	Thickness	Lithology	Paleo-strata thickness	Effective source rock thickness	TOC (%)		Evaluation
						min—max	Average (Number of samples)	
977-1369	K	392	Dark mud-rock	0	0	0.05—0.54	0.10 (25)	Non-source
1369-1698	K	329	Tuff	33	0	0.06—0.30	0.15 (6)	Non-source
			Dark sandy mud-rock	45.5	0	0.06—0.11	0.08 (15)	Non-source
			Tuff	215	0	0.14—0.63	0.27 (28)	Non-source
1698-2412	J_{2+3}	713	Dark sandy mud-rock	529.38 (with tuff and sandstone reduced)	82.87	0.5—1.15	0.70 (36)	Poor-moderate source
					46.16	1—1.48	1.32 (11)	Moderate to good source

2.2. Reservoir conditions

According to the formations revealed by well LF35-1-1 and seismic data interpretation, there may be two sets of reservoirs in the Chaoshan Depression. One set is the continental river-lake sandstone reservoir in Cretaceous, and the other set is coastal-shallow sea sandstone, slope fan and basin-bottom fan sandstone in the Upper-mid Jurassic, and sandstone and limestone reservoirs in transgresses system tracts.

The seismic profile (Figure 2) across structure B shows that a set of limestone layers with stable thickness are distributed on the top of the Middle Jurassic (T_{j2} interface). A set of submarine fan sandstones advancing from SE to NW are developed on the top of the Upper Jurassic. The fan root (inner fan and levee deposits) is located on southeast of the profile. And mid-fan mainly develops in middle and northwest with mid-fan channel deposits, where there are sandstone reservoirs of the best properties. Mid-fan frontal deposits develop in northwest.

Vertically on the seismic profile, the down lap characteristics of the fore set can be clearly seen from SE to NW. The submarine fan can be divided into four stages, among which the second and third are most flourishing, and it is speculated that the sand content is the largest (Figure 3). Laterally, the results of seismic facies analysis show that the submarine fan is distributed in SE-NW direction, and structure B is located in braided channels and non-channel of the mid-fan area, where sandstone reservoirs of good quality develop.

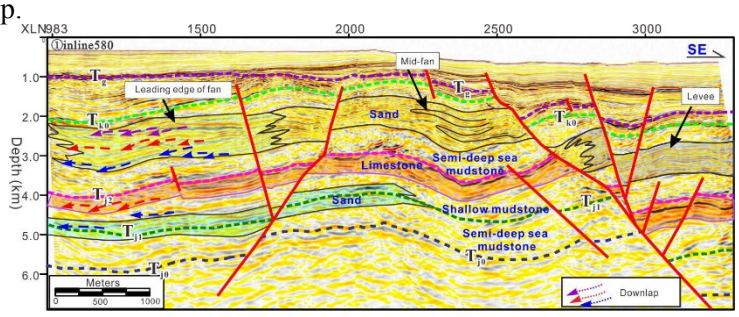

Figure 2. Seismic facies interpretation profile for reservoirs of structure B.

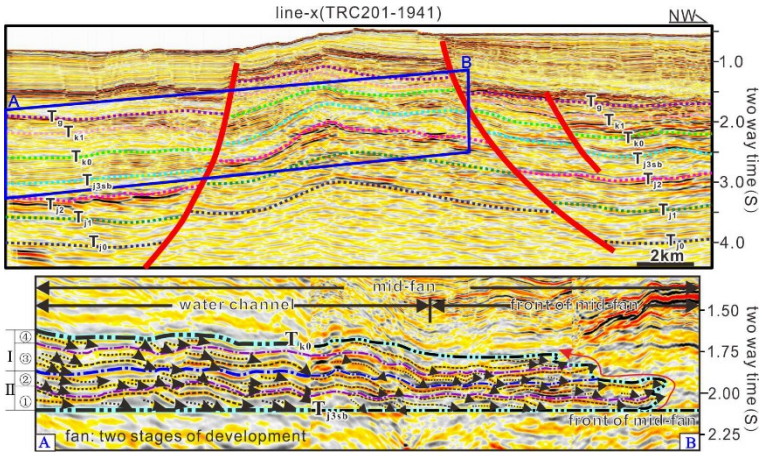

Figure 3. Detailed interpretation for upper-Jurassic fan of structure B.

2.3. Seal conditions

According to well LF35-1-1, multiple layers of mudstones encountered in this well are thick, and the maximum thickness of individual layer is more than 30 m. They should have good sealing capabilities and serve as important regional cap rocks in the area. In addition, there are many sets of mudstones in the Middle-Upper Jurassic, and these mudstones are mostly characterized of continuous or poorly

continuous, medium or weak amplitude reflections on the seismic profile. According to the seismic profile, the distribution of these strata is stable, which can also serve as a regional cap rock.

2.4. Reservoir-forming model

According to cores of well LF35-1-1, the Cretaceous and Middle-Upper Jurassic are mostly composed of interbedded sand-mudstone in the Chaoshan Depression, which is very favourable to form good reservoir-seal assemblage. The main accumulation mode is source-reservoir coincidence and reservoir overlaying source (Figure 4).

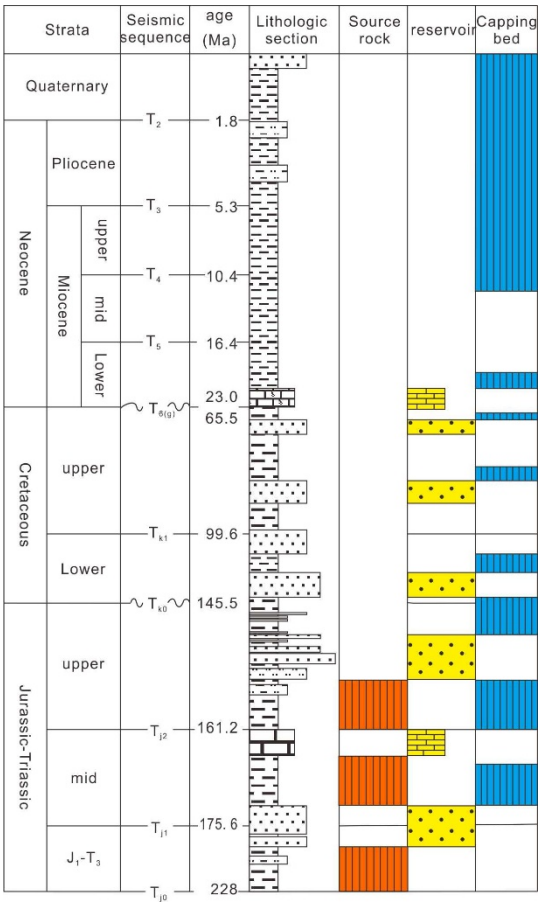

Figure 4. Main source-reservoir-seal assemblages in Chaoshan Depression.

3. Selected DHI techniques

3.1. Amplitude attribute of -90 degree phase component by phase decomposition

Phase decomposition is a unique and creative technology for DHI, originated by Castagna [17]. The acoustic impedance variations caused by pore fluids or lithology changes do not always produce very obvious amplitude anomalies on conventional post-stack profiles. By decomposing seismic traces into different phase components and suppressing unwanted phase components, it is possible to identify some subtle hydrocarbon, lithological changes or anomalous responses caused by sand channels, where significant amplitude anomalies occur at the expected phase components. This technology has become a very effective tool for special geological body identification and hydrocarbon detection [18-19].

Based on spectral decomposition [20], any seismic trace can be decomposed into 2D functions, amplitude spectrum and phase spectrum. A seismic trace S (t) is a 1D function whose amplitude varies with time. The amplitude spectrum A (f,t)is a 2D function whose amplitude varies with both time and frequency, and the phase spectrum θ(f, t) is a 2D function whose phase varies with time and frequency

also. If we combine the amplitude spectrum and the phase spectrum into a function A (f, t) * cosθ (f, t), then a two-dimensional function representing reflection amplitude changes with phase and time can be obtained by the following formula:

$$S'(\theta,t)=\int_{f_1}^{f_2} A(f,t)\cos\theta(f,t)df \quad (1)$$

Where f1 and f2 are the starting and ending frequencies of the band. We define this function as phase gather. Any desired phase component in the specified frequency band is extracted as follows:

$$S'(t)=\int_{\theta_1}^{\theta_2} S'(\theta,t)d\theta \quad (2)$$

Where θ1 and θ2 are the starting and ending phases of the phase band. In this way, the seismic reflection events with specific spectral characteristics can be suppressed or enhanced. The process of decomposing a seismic trace into a two-dimensional function of amplitude with time and phase is called phase decomposition. The amplitude change with time at a specific phase is referred to as a phase component. The seismic reflections caused by small impedance changes in the layer below the tuning thickness can be amplified, making specific geological features easier to discover. Any pair of reflection coefficients can be expressed as the sum of an odd and an even component. The reflection coefficients of even component are the same in size and sign, and those of odd component are the same in size and opposite in sign. As to an individual thin layer, the impedance variation changes the reflectivity of odd component, and thus the phase of the local reflectivity, while the even component remains almost unchanged. A phase filter can be designed and applied to seismic data based on the method described above, and the odd component may show an obviously strong amplitude anomaly at the location where weak amplitude appears originally. Especially in the case of low-impedance thin gas or light oil sands (bright spots), the amplitude abnormality corresponding to gas saturation will appear in the -90 degree phase component. Therefore, in practical applications, amplitude attribute analysis of -90 degree phase component is often used as a means for DHI.

Based on this technology, oil layer prediction is successfully carried out in EBS field in southeast Baghdad, Iraq. The primary layer of EBS oilfield for development is the Z5-Z6 sandstone reservoirs, which have obtained high-rate oil flow. However, the reservoir heterogeneity is strong, the sand-bodies are difficult to co-relate laterally, and the reservoir prediction is difficult. The controlling factors and the types of oil accumulation are unclear, and DHI is difficult. For this set of reservoirs, phase decomposition technology is used to for DHI, and a number of drilled wells confirm the reliability of the technology.

The figure on the left is the minimum amplitude map (Figure 5). According to this map, the reservoir distribution is stable with a good continuity. Using phase decomposition technique, the -90 degree phase amplitude attribute map is extracted (Figure 5 on the right). According to the map, the reservoir range is obviously reduced, and at the same time, the local continuity is deteriorated, and the oil accumulation range is significantly reduced. Well EB-B is the first newly drilled based on the prediction map and post-drilling results are consistent with the predicted results. The oil layer thickness is about 12m, equivalent to that of the early well EB02., Other four wells (Z-1, Z-2, Z-3 and Z-4) are drilled one after another afterwards, among which Z-2 and Z-3 are better in production. However Z-1 and Z-4 are located at the edge of the anomaly on the attribute map, and only the 2-3m oil layer is encountered with poor oil-bearing property, although the sand reservoirs are well developed.

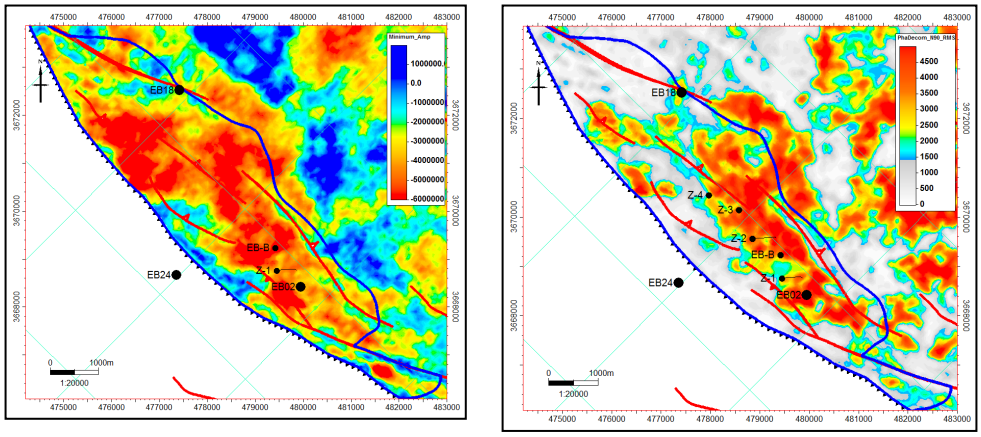

The minimum amplitude map of layer Z5-Z6 in EB02 well area

-90 degree phase amplitude map of layer Z5-Z6 in EB02 well area

Figure 5. Comparison of the minimum amplitude map and -90 degree phase amplitude map of layer Z5-Z6 in EB02 well area.

3.2. Spectral decomposition peak amplitude analysis

The peak amplitude attribute is an important one by spectral decomposition, and it is the maximum value of the reflection coefficient amplitude spectrum after eliminating the tuning effect [21]. Over the time domain amplitude attribute, it has the advantage to reflect the changes reservoir properties and hydrocarbon accumulations more realistically.

According to Castagana, any pair of reflection coefficients can be decomposed into odd and even parts (Figure 6). The odd component ro is composed of reflection coefficients with opposite amplitudes and polarities, while the even odd component re is composed of reflection coefficients with equal amplitude values and the same polarities.

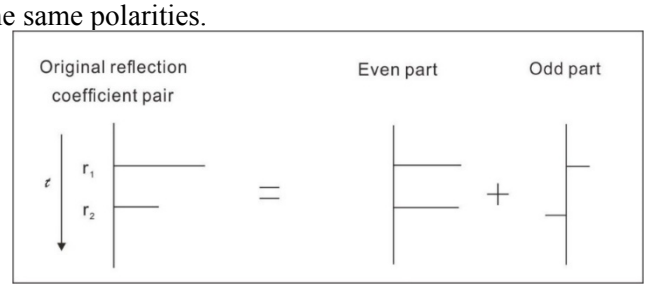

Figure 6. The decomposition of a reflectivity pair into an even and an odd pair.

With Fourier transform, the reflection coefficient expression is represented in frequency domain:

$$G(f) = 2r_e \cos(\pi fT) + i2r_o \sin(\pi fT)$$

Then the amplitude spectrum expression of the reflection coefficient pair is obtained:

$$A[G(f)] = [(r_1 + r_2)^2 \cos^2(\pi fT) + (r_1 - r_2)^2 \sin^2(\pi fT)]^{\frac{1}{2}}$$

The peak amplitude attribute is the maximum value of the amplitude spectrum expression. From the calculation formula of the amplitude spectrum, it can be seen that for a set of layers, changes in fluid or lithology or reservoir properties will increase absolute values of the top and bottom reflection coefficients, which is reflected by the significantly increased peak amplitude attribute [22].

In practical application in this area, the peak amplitude attribute can be obtained to directly detect reservoir and oil-bearing properties. The original seismic profile and peak amplitude attribute are displayed in Figure 7 and 8 respectively. It is difficult to distinguish the oil and brine layer directly on

the conventional amplitude profile since the amplitude of the brine layer and the oil layer is not much different. While on peak amplitude attribute profile, the oil layer is characterized of strong amplitude and the oil layer is characterized by weak reflection. The peak amplitude attribute can be used to effectively distinguish oil layers.

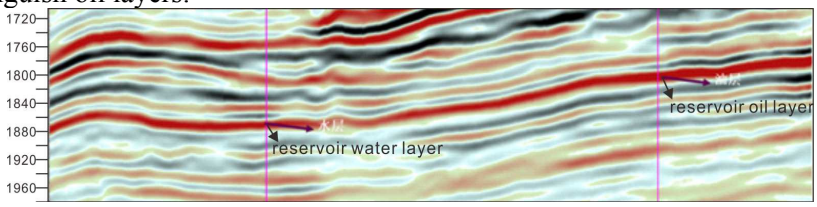

Figure 7. Original seismic section.

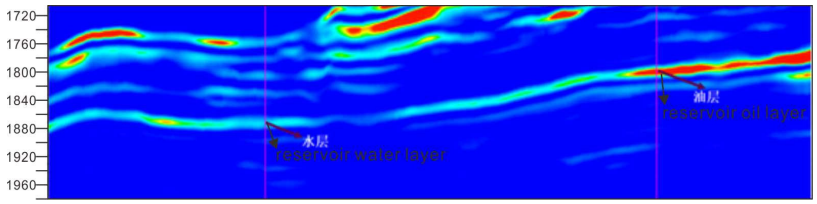

Figure 8. Peak amplitude attribute section.

4. Selected DHI techniques

-90 degree phase component technology for DHI has achieved excellent results in practical applications. In the exploration target area of Chaoshan Depression, there is no well drilled available. It is wondered that the technique of phase decomposition and -90 degree phase component DHI can achieve good results. We conduct forward modeling using the reservoir properties adjacent to the Chaoshan Depression to see what will happen to the amplitude attribute of -90 degree phase component if target reservoir contains oil and gas, and whether it can predict oil and gas.

4.1. Model establishment

The main purpose of establishing the forward model is to investigate the response characteristics of the amplitude of the -90 degree phase component to oil, gas or brine. The forward modeling is implemented using Leonardo technology and then the response characteristics of the two attributes with different pore fluids are summarized.

In practical work, there are three types of impedance changes for reservoir and its surrounding rocks: ① The impedance of surrounding rocks is higher than that of oil, gas or brine reservoirs, and oil-gas reservoirs are characterized of bright spots; ② The impedance of surrounding rock is lower than that of oil, gas or brine reservoirs, and oil-gas reservoirs is characterized of dim spots; ③ The impedance of surrounding rock is lower than that of brine-bearing reservoirs, but higher than that of oil-gas reservoirs, which shows polarity reversal (Figure 9).

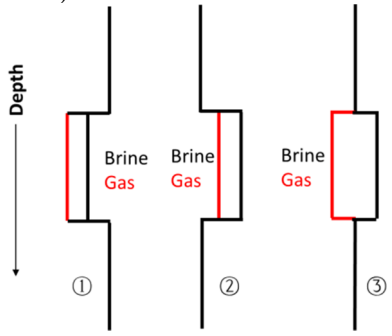

Figure 9. Assemblage patterns of reservoir and surrounding rocks.

According to the above assemblage patterns for reservoir and the surrounding rocks, and the drilling data of well LF35-1-1 in northern slope, the geological model is established firstly according to the lithology combination and velocity changes in the target area. The upper Jurassic stratum is the target zone, with a depth of about 1700-2300 meters. The lithology of the overlying rocks includes siliceous rock, mudstone, and argillaceous siltstone; and the reservoir lithology includes sandstone, siltstone; and underlying rocks is limestone. Various lithology and its velocity are as follows in Table 2.

Table 2. Rock types and their velocities listed.

Lithology	Depth (m)	Velocity (m/s)
Siliceous rock	1700-1900	5350
Mudrock	1950-2080	4200
Shaly siltstone and siltstone	1900-1950 2080-2200	5250
Limestone	2200-2300	5450

According to the velocity characteristics of siliceous rock and mudstone, the following three models are established (Figure 10-12). For No. 1 model, the overlying rock is siliceous rock with velocity of 5350m/s, which is greater than that of the sandstone reservoir. For No. 2 model, the overlying rock is mudstone, and its velocity of 4200 m/s is less than that of sandstone reservoir. As to No. 3 model, the overlying rock is a combination of siliceous and mudstone with the velocity of 5100m/s, which is the average velocity of siliceous rocks and mudstones, and the caprock velocity are close to that of the sandstone reservoir.

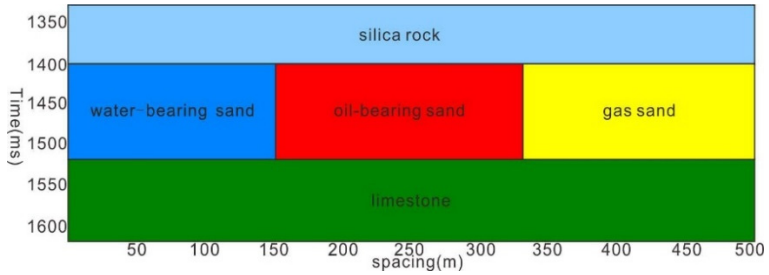

Figure 10. Lithology assemblage No. 1 model.

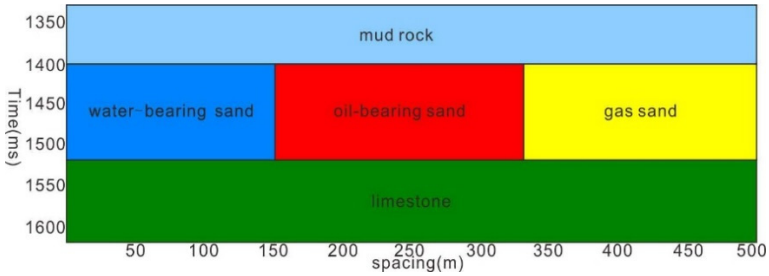

Figure 11. Lithology assemblage No. 2 model.

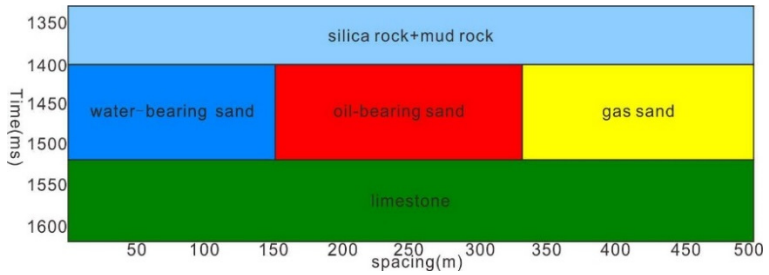

Figure 12. Lithology assemblage No. 3 model l.

4.2. Seismic modeling for DHI in Chaoshan Depression

The forward seismic profiles corresponding to the three models are displayed in Figures 13-15. According to the synthetic profiles by forward modeling, the reservoir top of model 1 is a trough, and the amplitude of oil/gas-bearing case is significantly higher than the brine-bearing reservoir. The reservoir top of model 2 is a peak reflection, and the amplitude when oil/gas-bearing case is significantly lower than brine-bearing case reservoir. The brine layer top of model 3 is a peak reflection, and the gas layer is a trough. The amplitude of the brine layer is slightly different from the gas layer, and the oil layer is a peak of weak amplitude. On seismic sections, it difficult to directly identify the oil and gas layer.

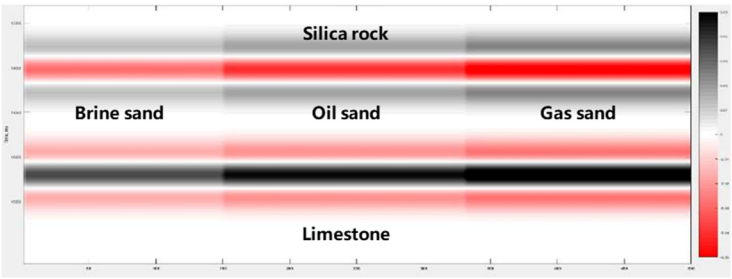

Figure 13. Synthetic section of model 1.

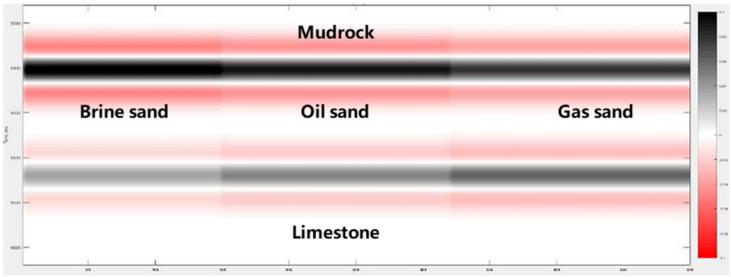

Figure 14. Synthetic section of model 2.

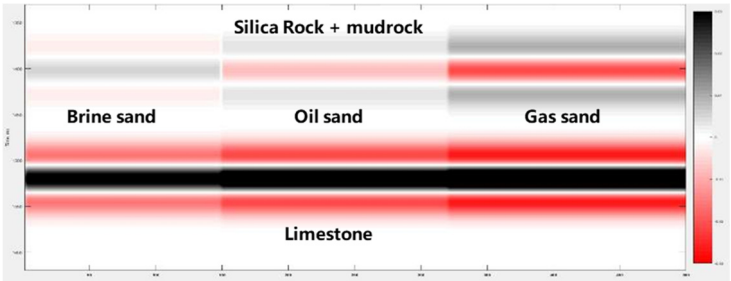

Figure 15. Synthetic section of model 3.

The amplitude attribute of the -90 degree phase component is extracted on forward synthetic seismic data (Figure 16-Figure 18). On -90o phase component profiles of the three models, it is similar that the gas layer has the strongest amplitude and brine layer the weakest amplitude, and the oil layer amplitude between gas and brine.

In Table 3, the absolute amplitude values of synthetic seismic data and -90 degree phase attributes are read from the three models of brine, oil and gas respectively. And amplitude values of -90 degree phase attributes are cross-plotted against those of synthetic seismic data (Figure 19). On the cross-plotting, there is not a uniform threshold to identify oil and gas layers for original synthetic seismic amplitude only, while for -90 degree phase amplitudes, uniform thresholds can be seen between brine and oil and gas. The amplitude value above 0.0005 is gas layer, and the amplitude between 0.0035-0.0005 oil layer, and the amplitude less than 0.00035 brine layer.

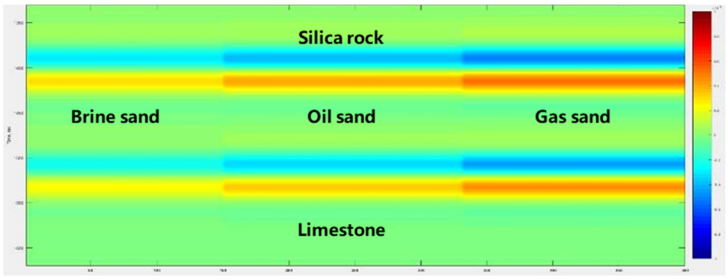

Figure 16. -90° phase component section of model 1 synthetics.

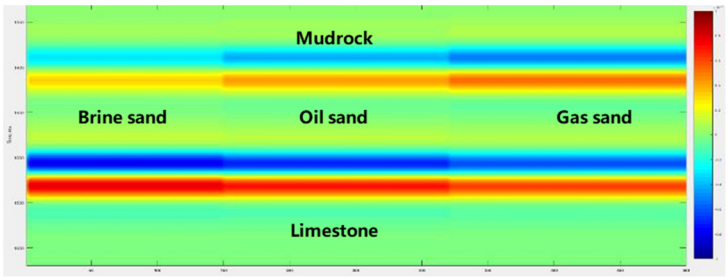

Figure 17. -90° phase component section of model 2 synthetics.

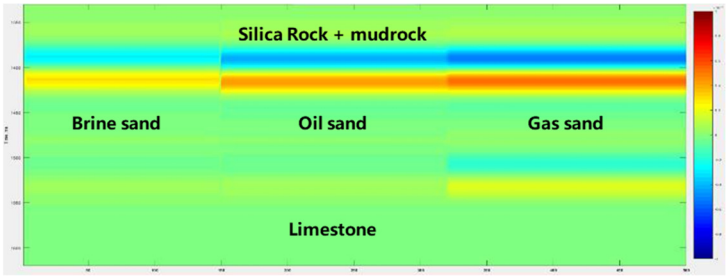

Figure 18. -90° phase component section of model 3 synthetics.

Table 3. Synthetic amplitudes and its phase component for different pore fluids cases.

Model	Fluids	Absolute amplitude of synthetic data	Absolute amplitude of -90 degree phase component
No. 1	Gas	0.053	0.00051
	Oil	0.041	0.00041
	Water	0.028	0.00031
No. 2	Gas	0.078	0.00052
	Oil	0.092	0.00042
	Water	0.11	0.00032
No. 3	Gas	0.021	0.00052
	Oil	0.0078	0.00043
	Water	0.0052	0.00028

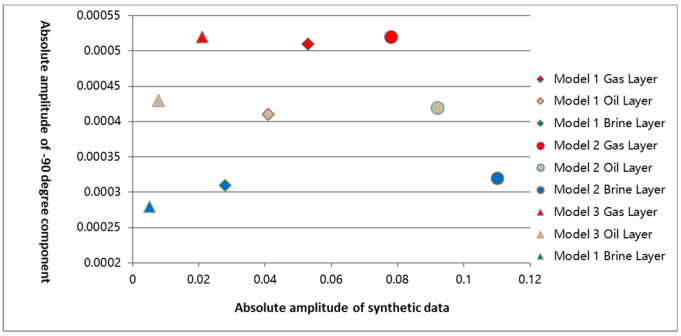

Figure 19. Cross plotting for synthetic amplitudes and its phase component of 3 models.

5. DHI for identification of exploration targets in Chaoshan Depreession

Well LF35-1-1 confirms that there are two sets of reservoir-cap rock assemblages in the Chaoshan Depression. One is interbedded sandstone and mudstone in Cretaceous, the other is the Middle-Upper Jurassic. And the latter is the main target interval for oil and gas exploration. For this main exploration target, the reservoir occurrence is analyzed by extracting conventional seismic amplitude attributes. DHI is performed using -90 degree phase component amplitude attribute analysis and spectrum decomposition peak amplitude attribute analysis respectively, so as to verify the two prediction results mutually and increase DHI confidence.

5.1. Analysis of conventional seismic amplitude attributes

Seismic amplitude attributes can indicate reservoir property variations to a certain extent, so the seismic amplitude attributes are usually applied to qualitatively analyze reservoir development. The seismic section along one favorable exploration target in the Chaoshan Depression is shown in Figure 20. On the section, the ZOI of Upper Jurassic shows strong reflections locally, which is probably the seismic response of the reservoir with better properties. By extracting its amplitude attribute, the lateral distribution range of the strong reflection of ZOI is preliminarily delineated, which probably corresponds to the range of favorable reservoirs of ZOI (Figure 21).

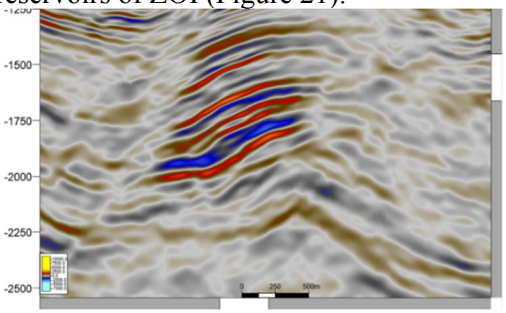

Figure 20. Original seismic section around ZOI.

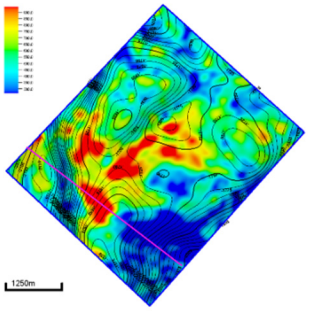

Figure 21. Original seismic amplitude attribute map extracted along ZOI.

5.2. -90 degree phase component amplitude attribute analysis for DHI

The -90 degree phase component amplitude attribute by phase decomposition for DHI is used to study on the seismic section where there are strong reflections around ZOI, to clarify the distribution of abnormal amplitudes of the -90 degree phase component attribute, and then to identify its possible oil and gas distribution scope.

A comparison between the original seismic profile and the -90 degree phase component profile is illustrated in Figure 22. From this comparison, strong amplitude reflections on the -90 degree phase component profile do not coincide with all those on the conventional seismic profile, and some strong amplitudes are no longer strong on -90 degree phase component profile. According to the previous forward modeling results, strong amplitudes on the -90 degree phase component profile is probably caused by presence of oil and gas. By extracting the amplitude attribute of the -90 degree phase component, the possible oil and gas distribution range is identified in Figure 23 on the right.

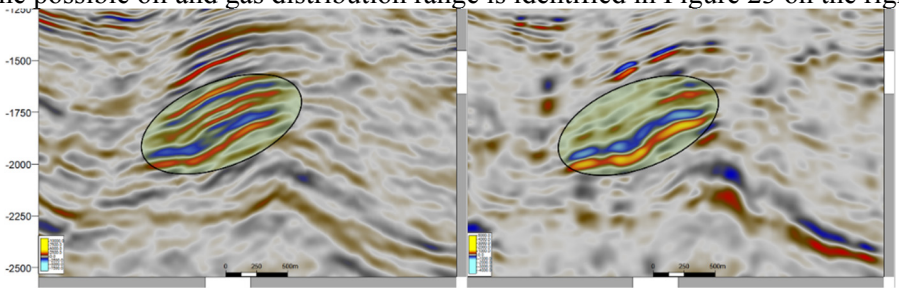

Figure 22. The seismic section (left) and -90 degree phase component section (right) of Up-Jurassic reservoir.

The comparison between the attribute map of conventional amplitude and that of -90 degree phase component along ZOI is illustrated in Figure 23. There are clusters of strong amplitude characteristics on both maps. However, the strong amplitude range on the -90-degree phase component map is reduced, and the boundary of the strong amplitude range is clearer, and it is more consistent structural contours. Obviously stronger amplitudes of -90-degree phase component especially occur on structural highs (Figure 23, on the right). Therefore, it is speculated that the oil and gas accumulation is extremely likely to occur in the areas with high amplitudes.

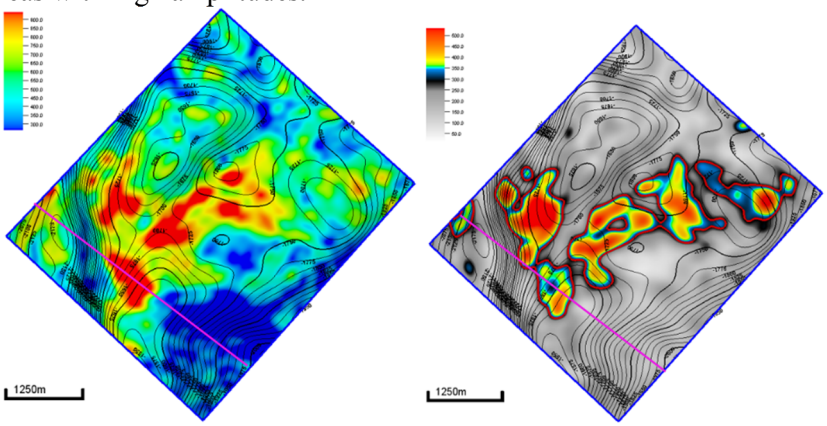

Figure 23. The attribute map (left) and -90 degree phase component map (right) of Up-Jurassic reservoir.

5.3. Spectral decomposition peak amplitude analysis for DHI

The peak amplitude attribute is sensitive to reservoir oil and gas. By comparing the original seismic section with the peak amplitude attribute section, it is found that oil/gas-bearing reservoirs show strong amplitude characteristics on the peak amplitude attribute section. A comparison between original

seismic section and the peak amplitude attribute section of favorable exploration targets in Chaoshan Depression is illustrated in Figure 24. The peak frequency amplitude section shows strong reflections locally, but the continuity varies slightly on the top. By comparing peak amplitude attribute map with the original amplitude attribute (Figure 25), the intensity of the peak amplitude attribute anomalies has slight changes laterally, and their continuity in anomalous areas fluctuates slightly. It also indicates that hydrocarbon accumulation scope is smaller than reservoir distribution range.

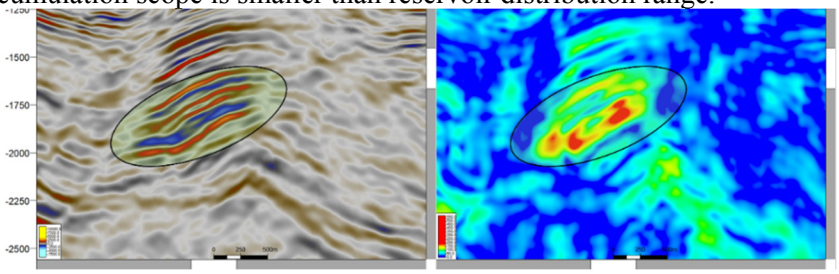

Figure 24. The seismic section (left) and peak amplitude section (right) of Up-Jurassic reservoir.

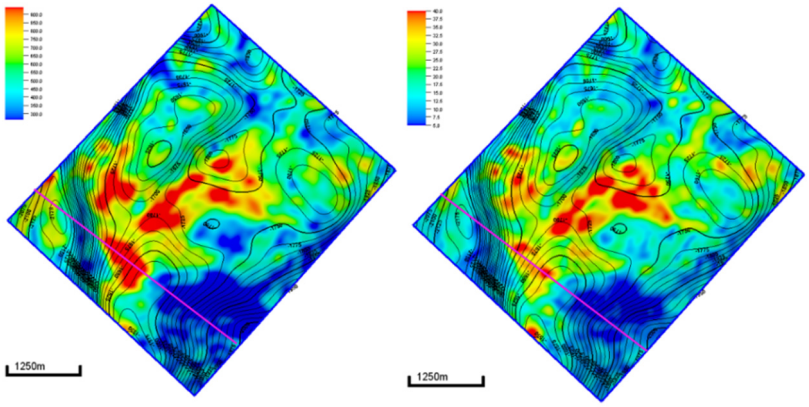

Figure 25. The attribute map (left) and peak amplitude map (right) of Up-Jurassic reservoir.

6. Conclusions

For exploration frontier areas under study, there is much uncertainty to apply conventional seismic attribute analysis for identifying oil and gas prospective targets due to few wells available. Fortunately, the joint application of two methods, -90 degree phase component amplitude attribute analysis by phase decomposition and peak amplitude attribute by spectrum decomposition, is an effective alternative for DHI in these areas. Together with its forward modeling analysis, -90 degree phase component amplitude attribute analysis method is used to predict reservoir oil and gas bearing property of the structure B in Chaoshan Depression, which indicates that there are probably oil-bearing layers in Upper Jurassic reservoirs. At the same time, it is supported by peak amplitude attribute analysis, and thereby the confidence of DHI results is enhanced.

References

[1] Liu G D 2001 The second exploitation of the oil and gas resources in China [J]. *Progress in Geophysics*, **16(4)**: 1-3.
[2] Zhang J Y, SUN Z, Zhang S F 2014 Analysis of Mesozoic tectonic deformation in the Chaoshan Depression of Pearl River Mouth Basin [J]. *Journal of Tropical Oceanography*, **33(5)**: 41-49.
[3] Hao H J, Lin H M, Yang M X, et al. 2001 The Mesozoic in Chaoshan depression: A new domain of petroleum exploration. *China Offshore Oil and Gas (in Chinese)*, **15(3)**: 157-163.
[4] Wang L L, Cheng R H, LI F, et al. 2009 The Mesozoic Sedimentary Sequences, Correlation and Geological Significance for Petroleum of the North Margin of South China Sea [J]. *Journal of*

Jilin University (Earth Science Edition), **39(2)**: 175-182.
[5] Zhang L, Geng A s, Wang LL, et al. 2012 Assessment of Mesozoic source rocks at The Margin of South China Continent [J]. *Marine Geology & Quaternary Geology*, **32(1)**: 99-108.
[6] Ji Z Y, Zhao H Q, et al. 2014 The Mesozoic Petroleum System of Chaoshan depression. *Petroleum Geology and Enginerering*, **28(3)**: 9-15.
[7] Wang P, Xia K Y, Huang C L 2000 The Mesozoic Marine sediment distribution and Geology-Geophysics characteristic at the North-Eastern of South China Continent [J]. *Journal of Tropical Oceanography*, **19(4)**: 28-35.
[8] Duan J C, Mi H F 2012 Seismic Facies and Sedimentary Facies study of Mesozoic in Chaoshan Sag [J]. *Resources & Industries*, **14(1)**: 100-105.
[9] Hao H J, Wang R L, Zhang X T, et al. 2004 Mesozoic marine sediment identification and distribution in the eastern Pearl River Mouth Basin. *China Offshore Oil and Gas*, **16(2)**: 84-88.
[10] Zhang Q L, Zhang H F, Zhang X T, et al. 2018 The upper Cretaceous prototype basin of the Chaoshan depression in the northern South China Sea and its tectonic setting [J]. *Chinese Journal of Geophysics*, vol **61(10)**: p4308-4321.
[11] Zhou D, Chen H Z，Sun Z, et al. 2005 Three Mesozoic sea basins in the eastern and southern South China Sea and their relation to Tethys and Paleo-Pacific domains. *Journal of Tropical Oceanography*, **24(2)**: 16-25.
[12] Yao B C, Zhang L, Wei Z Q, et al. 2011 The Mesozoic Tectonic Characteristics and Sediment Basins in the Eastern Margin of South China Continen [J]. Marine Geology & Quaternary Geology, **31(3)**:47-60.
[13] Zhong G J, Wu S M, Feng C M 2011 Sedimentary model of Mesozoic in the northern South China Sea. *Journal of Tropical Oceanography*, **30(1)**: 43-48.
[14] Hao H J, Shi H S, Zhang X T, et al. 2009 Mesozoic sediments and their petroleum geology conditions in Chaoshan sag: A discussion based on drilling results from the exploratory well LF35-1-1. *China Offshore Oil and Gas (in Chinese)*, **21(3)**: 151-156.
[15] Zhong G J, Yi H, Lin Z, et al. 2007 Characteristic of Source Rocks and Mesozoic in Continental Slope Area of Northeastern the South China Sea and East Guangdong of China. *XINJIANG Petroleum Geology*, **28 (6)**: 676-680.
[16] Yang S C, Tong Z G, He Q, et al. 2009 Mesozoic hydrocarbon generation history and igneous intrusion impacts in Chaoshan depression, South China Sea: A case of LF35-1-1 well. *China Offshore Oil and Gas (in Chinese)*, **20(3)**: 152-156.
[17] Castagna J, Oyem A, Portniaguine O and Aikulola U 2016 Phase decomposition: Interpretation, 4, no. 3, SN1–SN10, doi: 10.1190/INT-2015-0150.1.
[18] Elita Selmara De Abreu, John Patrick Castagna and Gabriel Gil 2018 Case study: Phase-component amplitude variation with angle: Geophysics, 84, B285–B297, doi: 10.1190/GEO2018-0762.1.
[19] Barbato U, Portniaguine O, Winkelman B and Castagna J 2017 Phasedecomposition as a DHI in bright-spot regimes: A Gulf of Mexico casestudy: 87th Annual International Meeting, SEG, Expanded Abstracts, 3976–3980, doi: 10.1190/segam2017-17737608.1.
[20] Partyka G, Gridley J and Lopez J 1999 Interpretational applications ofspectral decomposition in reservoir characterization: The Leading Edge, 18, 353–360.
[21] Barnes A E 1993 Instantaneous spectral bandwidth and dominantfrequency with applications to seismic reflection data: Geophysics, 58, 419–428, doi: 10.1190/1.1443425.
[22] Bracewell, R. N., 1978 The Fourier Transform and its applications: McGraw-Hill.